Ta^{5+} Displacements in $CsTaQ_3$ (Q = S, Se, and Te): New One-Dimensional Materials with the $BaVS_3$ Structure

Michael A. Pell,[†] Grigori V. M. Vajenine,[‡] and James A. Ibers*,[†]

Contribution from the Departments of Chemistry, Northwestern University, Evanston, Illinois 60208-3113, and Cornell University, Ithaca, New York 14853-1301

Received December 31, 1996[⊗]

Abstract: The new compounds $CsTaQ_3$ (Q = S, Se, and Te) have been synthesized through stoichiometric reactions of the elements with Cs_2Q_n reactive fluxes at 923 K. Their crystal structures have been determined by single-crystal X-ray methods. $CsTaQ_3$ crystallize in the hexagonal space group D_{6h}^4−$P6_3/mmc$ with two formula units per cell. Crystal data: $CsTaS_3$, a = 7.266(2) Å, c = 5.961(2) Å, V = 272.55(10) Å^3 (T = 115 K), $R_w(F^2)$ = 0.072 (NO = 114, NV = 11), R_1 = 0.034; $CsTaSe_3$, a = 7.500(1) Å, c = 6.182(1) Å, V = 301.15(7) Å^3 (T = 115 K), $R_w(F^2)$ = 0.106 (NO = 112, NV = 11), R_1 = 0.036; $CsTaTe_3$, a = 7.992(4) Å, c = 6.496(4) Å, V = 359.3(4) Å^3 (T = 115 K), $R_w(F^2)$ = 0.131 (NO = 111, NV = 10), R_1 = 0.038. The compounds adopt the $BaVS_3$ structure type and feature $^1_\infty[TaQ_3^-]$ chains of face-sharing octahedra. The Ta^{5+} centers are displaced from the centers of the Q_6 octahedra along the direction of the chains in a centrosymmetric fashion. Geometrical considerations and band structure calculations at the extended Hückel and density functional (DFT) levels of theory suggest that the most likely distortion pattern is the one with all Ta^{5+} centers displaced in the same direction within a given chain. A second-order Jahn−Teller effect is responsible for this distortion. Very weak interchain communication would result in a centrosymmetric structure. The chains are separated by 12-coordinate Cs^+ cations. $CsTaSe_3$ is an insulator. $CsTaTe_3$ shows semiconducting behavior and is diamagnetic or weakly paramagnetic. Differential scanning calorimetry (DSC) and high-temperature powder diffraction data indicate that $CsTaTe_3$ undergoes a phase transition at ≈493 K.

Introduction

The literature of ternary alkali-metal and alkaline-earth-metal group-V chalcogenides is dominated by the A_xMQ_2 layered intercalation compounds (A = Li, Na, K; M = Nb, Ta; Q = S, Se.[1] A = Cs, Rb; M = Nb; Q = S[2]), the one-dimensional materials $BaM_{0.8}Q_3$ (M = Nb; Q = S. M = Ta; Q = Se[3,4]), and $BaMQ_3$ (M = V; Q = S,[5−7] Se.[8] M = Nb; Q = S.[4] M = Ta; Q = S,[9] Se[10,11]). However, other interesting phases exist. K_3MQ_4 (M = Nb, Ta; Q = S, Se[12]) contains isolated MQ_4^{3-} tetrahedra whereas $K_3Nb_2Se_{11}$ and $K_4Ta_2S_{11}$[13] comprise pairs of seven-coordinate Nb and Ta polyhedra with extensive chalcogen−chalcogen bonding. Although a variety of complex barium group-V sulfides are known,[14−19] prior to the present work no ternary alkali-metal or alkaline-earth-metal group-V tellurides had been characterized. It was anticipated that a low-temperature reaction that involved Te, the least electronegative chalcogen, would favor the formation of a cluster compound with chalcogen−chalcogen interactions, as in $K_3Nb_2Se_{11}$. With this intention we have extended this ternary system to include the tellurides. Upon the discovery of a new compound possessing the $BaVS_3$ structure type, namely $CsTaTe_3$, we set out to synthesize the analogous sulfide and selenide compounds. Here we report the syntheses, crystal structures, and some physical properties of $CsTaQ_3$ (Q = S, Se, and Te). Through the use of the extended Hückel method we present a qualitative rationalization of the observed displacements of Ta atoms from the centers of TaQ_6 octahedra in $CsTaQ_3$. DFT calculations are also used to address the Ta displacements.

Experimental and Theoretical Section

Syntheses. $CsTaQ_3$ (Q = S, Se, and Te) were synthesized by the reactive-flux method.[20] Elemental S (Johnson Matthey, 99.999%), Se (Aldrich, 99.5%), and Te (Aldrich, 99.8%) were stoichiometrically added to Cs (Aldrich, 99.5%) dissolved in liquid NH_3 at 194 K to form Cs_2S_5, Cs_2Se_3, and Cs_2Te_3, respectively. Cs_2Q_n was then ground together with powders of Ta (Aldrich, 99.9%) and Q in a 1:2:1 ratio for Q = S and a 1:2:3 ratio for Q = Se and Te and sealed under high vacuum in fused-silica tubes. The charged tubes were heated at 923 K for 6 d, then cooled to room temperature at 4 K/h. Black

[†] Northwestern University.
[‡] Cornell University.
[⊗] Abstract published in *Advance ACS Abstracts,* May 1, 1997.

(1) Omloo, W. P. F. A. M.; Jellinek, F. *J. Less-Common Met.* **1970**, *20*, 121−129.
(2) Chen, Bai-H.; Eichhorn, B.; Peng, Jian-L.; Greene, R. L. *J. Solid State Chem.* **1993**, *103*, 307−313.
(3) Donohue, P. C.; Weiher, J. F. *J. Solid State Chem.* **1974**, *10*, 142−144.
(4) Kim, Sung-J.; Bae, Hyun-S.; Yee, Kyeong-A.; Choy, Jin-H.; Kim, Dong-K.; Hur, Nam-H. *J. Solid State Chem.* **1995**, *115*, 427−434.
(5) Gardner, R. A.; Vlasse, M.; Wold, A. *Acta Crystallogr., Sect. B: Struct. Crystallogr. Cryst. Chem.* **1969**, *25*, 781−787.
(6) Kelber, J.; Jorgensen, J. D.; Mueller, M. H. *Acta Crystallogr., Sect. B: Struct. Crystallogr. Cryst. Chem.* **1979**, *35*, 2473−2475.
(7) Ghedira, M.; Chenavas, J.; Sayetat, F.; Marezio, M.; Massenet, O.; Mercier, J. *Acta Crystallogr., Sect. B: Struct. Crystallogr. Cryst. Chem.* **1981**, *37*, 1491−1496.
(8) Kelber, J.; Reis, A. H., Jr.; Aldred, A. T.; Mueller, M. H.; Massenet, O.; DePasquali, G.; Stucky, G. *J. Solid State Chem.* **1979**, *30*, 357−364.
(9) Aslanov, L. A.; Kovba, L. M. *Russ. J. Inorg. Chem.* **1964**, *9*, 1317−1319.
(10) Aslanov, L. A. *Russ. J. Inorg. Chem.* **1964**, *9*, 1090−1091.
(11) Gardner, R. A.; Vlasse, M.; Wold, A. *Inorg. Chem.* **1964**, *8*, 2784−2787.
(12) Latroche, M.; Ibers, J. A. *Inorg. Chem.* **1990**, *29*, 1503−1505.
(13) Schreiner, S.; Aleandri, L. E.; Kang, D.; Ibers, J. A. *Inorg. Chem.* **1989**, *28*, 392−393.
(14) Saeki, M.; Onoda, M. *Mater. Res. Bull.* **1989**, *24*, 41−47.
(15) Onoda, M.; Saeki, M. *Mater. Res. Bull.* **1989**, *24*, 625−631.
(16) Saeki, M.; Nozaki, H.; Onoda, M. *Mater. Res. Bull.* **1989**, *24*, 851−858.
(17) Saeki, M.; Onoda, M. *Mater. Res. Bull.* **1989**, *24*, 1491−1499.
(18) Saeki, M.; Onoda, M. *Mater. Res. Bull.* **1990**, *25*, 723−730.
(19) Saeki, M.; Nozaki, H.; Onoda, M. *J. Alloys Compd.* **1996**, *234*, 178−182.
(20) Sunshine, S. A.; Kang, D.; Ibers, J. A. *J. Am. Chem. Soc.* **1987**, *109*, 6202−6204.

S0002-7863(96)04473-3 CCC: $14.00

Table 1. Crystal Data and Intensity Collection for $CsTaQ_3$ (Q = S, Se, and Te)

formula	$CsTaS_3$	$CsTaSe_3$	$CsTaTe_3$
formula mass (amu)	410.04	550.74	696.66
space group	$D_{6h}^4-P6_3/mmc$	$D_{6h}^4-P6_3/mmc$	$D_{6h}^4-P6_3/mmc$
a (Å)[a]	7.266(2)	7.500(1)	7.992(4)
c	5.961(2)	6.182(1)	6.496(4)
V (Å^3)	272.55(10)	301.15(7)	359.3(4)
Z	2	2	2
ρ_c (g cm^{-3})	4.996	6.074	6.439
temp of data collection (K)[b]	115(2)	115(2)	115(2)
radiation	graphite monochromated Mo Kα ($\lambda(K\alpha_1) = 0.7093$ Å)		
linear abs coeff (cm^{-1})	277	422	321
transmission factors[c]	0.309−0.487	0.448−0.529	0.343−0.392
λ^{-1} sin θ limits (Å^{-1})	0.079−0.595	0.077−0.571	0.072−0.628
no. of data collected	212	1822	1750
no. of unique data	114	112	111
$R_w(F^2)$[d]	0.072	0.106	0.131
R_1[d]	0.034	0.036	0.038

[a] Obtained from a refinement with the constraints $a = b$, $\alpha = \beta = 90°$, $\gamma = 120°$. [b] The low temperature system is based on a design by Huffman.[69] [c] The analytical method as employed in the Northwestern absorption program AGNOST was used for the absorption correction.[22] [d] $R_w(F_o^2) = [\sum[w(F_o^2 - F_c^2)^2]/\sum wF_o^4]^{1/2}$; $w^{-1} = \sigma^2(F_o^2) + (0.04F_o^2)^2$ for $F_o^2 \geq 0$; $w^{-1} = \sigma^2(F_o^2)$ for $F_o^2 \leq 0$; $R_1(F) = \sum||F_o| - |F_c||/\sum|F_o|$.

hexagonal needles of the title compounds were manually extracted from the reaction melts. Energy Dispersive X-ray (EDX) analyses confirmed the presence of Cs, Ta, and Q in 1:1:3 ratios. $CsTaTe_3$ is obtained as a pure phase, as established by X-ray powder diffraction studies. Although $CsTaS_3$ and $CsTaSe_3$ are the major phases produced under the reaction conditions reported, minor amounts of TaS_2 and $TaSe_2$ are invariably produced as well. Attempts to discover other phases in this system at lower reaction temperatures were unsuccessful. The compounds are stable in air for several months.

Structure Determinations. Laue symmetry 6/*mmm* and preliminary lattice constants were established from Weissenberg photographs obtained at room temperature. The systematic extinctions (*hhl*: $l = 2n + 1$) are consistent with the hexagonal space groups $C_{6v}^4-P6_3mc$, $D_{3h}^4-P\bar{6}2c$, and $D_{6h}^4-P6_3/mmc$. Final lattice constants were obtained from a least-squares analysis of the setting angles of reflections automatically centered with the use of Mo Kα radiation on a Picker diffractometer at 115 K ($CsTaS_3$: 24 reflections in the range 39−41°; $CsTaSe_3$: 35 reflections in the range 38−41°; $CsTaTe_3$: 18 reflections in the range 27−50°). In each structure determination six standard reflections monitored every 100 reflections showed no appreciable change in intensity throughout the data collection. The data were processed[21] and corrected for absorption.[22] Agreement among Friedel pairs strongly favored the centrosymmetric space group $P6_3/mmc$. The structure of $CsTaTe_3$ was solved in this space group by direct methods with the program SHELXS.[23] Positional parameters from the $CsTaTe_3$ structure were used as initial parameters for the refinements of the $CsTaS_3$ and $CsTaSe_3$ structures. The structures were refined with the use of the program SHELXL.[24] Refinements of $CsTaS_3$ and $CsTaSe_3$ included an extinction parameter. In each refinement the displacement parameter of atom Ta(1) in the [001] direction was unreasonably large. The atom was subsequently moved from the $\bar{3}m$ site (0,0,0) to a $3m$ site (0,0,z), and its z coordinate was refined with occupancy fixed at $^1/_2$. The improvement in the agreement indices is dramatic, suggesting that this model of Ta disorder has validity.[25] Details of the refinements are given in Table 1. Positional parameters and equivalent isotropic displacement parameters are given in Table 2. Selected bond lengths are provided in Table 3. Further details are available as Supporting Information.

Table 2. Positional Parameters and Equivalent Isotropic Displacement Parameters for $CsTaQ_3$ (Q = S, Se, and Te)

atom	x	y	z	Wyckoff notation	U(eq)[a] (Å^2)
$CsTaS_3$					
Cs(1)	$^1/_3$	$^2/_3$	$^3/_4$	2*d*	0.0143(6)
Ta(1)[b]	0	0	0.0337(10)	4*e*	0.025(2)
S(1)	0.1550(4)	0.3100(8)	$^1/_4$	6*h*	0.0199(11)
$CsTaSe_3$					
Cs(1)	$^1/_3$	$^2/_3$	$^3/_4$	2*d*	0.0203(10)
Ta(1)[b]	0	0	0.0446(4)	4*e*	0.0251(14)
Se(1)	0.1604(2)	0.3208(3)	$^1/_4$	6*h*	0.0216(10)
$CsTaTe_3$					
Cs(1)	$^1/_3$	$^2/_3$	$^3/_4$	2*d*	0.0256(13)
Ta(1)[b]	0	0	0.0506(4)	4*e*	0.021(2)
Te(1)	0.1642(2)	0.3284(3)	$^1/_4$	6*h*	0.0280(12)

[a] U(eq) is defined as one-third of the trace of the orthogonalized U_{ij} tensor. [b] Occupancy fixed at $^1/_2$.

Table 3. Selected Bond Lengths (Å) for $CsTaQ_3$ (Q = S, Se, and Te)

compd	Ta−Ta	Ta−Q	Cs−Q
$CsTaS_3$	2.579(12)[a]	2.339(5) × 3	3.636(1) × 6
	2.980(1)[b]	2.582(6) × 3	3.731(3) × 6
$CsTaSe_3$	2.540(2)[a]	2.440(2) × 3	3.751(1) × 6
	3.091(1)[b]	2.767(2) × 3	3.821(1) × 6
$CsTaTe_3$	2.590(6)[a]	2.616(3) × 3	3.996(2) × 6
	3.248(2)[b]	2.997(3) × 3	4.004(2) × 6

[a] Ta−Ta distance in the model with pairing distortion. [b] Ta−Ta distance in the model with ordered polar chains (sliding distortion).

Electrical Conductivity of $CsTaSe_3$ and $CsTaTe_3$. Four gold wires with graphite leads were attached along the needle axis ([001]) of single crystals of $CsTaSe_3$ and $CsTaTe_3$. Two-probe dc resistivity measurements were performed at room temperature and at 77 K.

Magnetic Susceptibility of $CsTaTe_3$. Magnetic susceptibility measurements were made as a function of both applied field and temperature with the use of a Quantum Design SQUID magnetometer on a 20-mg sample of $CsTaTe_3$. Sample integrity was established from an X-ray powder diffraction pattern. Field-dependence measurements were made at 6, 200, and 300 K over the range 2000 to 10000 G. Temperature-dependence measurements were made at 5000 G over the range 6 to 300 K. All measurements were corrected for background and for core diamagnetism.[26]

Thermal Measurements on $CsTaTe_3$. DSC measurements were performed on a DuPont Instruments 910 differential scanning calorimeter. The samples were hermetically sealed in Al cells. A heating

(21) Waters, J. M.; Ibers, J. A. *Inorg. Chem.* **1977**, *16*, 3273−3277.
(22) de Meulenaer, J.; Tompa, H. *Acta Crystallogr.* **1965**, *19*, 1014−1018.
(23) Sheldrick, G. M. SHELXTL PC Version 5.0, An Integrated System for Solving, Refining, and Displaying Crystal Structures from Diffraction Data. Siemens Analytical X-Ray Instruments, Inc.: Madison, WI, 1994.
(24) Sheldrick, G. M. *J. Appl. Crystallogr.* In preparation.
(25) Refinement with Ta at (0,0,0): U_{33}(Ta) = 0.0652, 0.1271, and 0.1925 Å^2 for $CsTaS_3$, $CsTaSe_3$, and $CsTaTe_3$, respectively. Refinement with Ta at (0,0,z): U_{33}(Ta) = 0.0150, 0.0170, and 0.0314 Å^2 for $CsTaS_3$, $CsTaSe_3$, and $CsTaTe_3$, respectively.
(26) Mulay, L. N.; Boudreaux, E. A., Eds. *Theory and Applications of Molecular Diamagnetism*; Wiley-Interscience: New York, 1976.

Table 4. Atomic Parameters Used in Extended Hückel Calculations

orbital		H_{ii} (eV)	z_1	z_2	c_1	c_2
Ta	6s	−10.10	2.28			
	6p	−6.86	2.241			
	5d	−12.10	4.762	1.938	0.6815	0.5774
S	3s	−20.0	2.112			
	3p	−11.0	1.827			
Se	4s	−20.5	2.44			
	4p	−14.4	2.07			
Te	5s	−20.8	2.51			
	5p	−14.8	2.16			
Cs	6s	−3.88	1.06			
	6p	−2.49	1.06			

rate of 5 K/min and a He flow rate of 40 mL/min were used. The instrument was calibrated with an In standard. Both temperature and the amount of heat were calibrated. Thermogravimetric analysis (TGA) measurements were obtained on a DuPont Instruments 951 TGA under similar conditions of heating rate and flow rate.

High-Temperature X-ray Powder Diffraction Study of $CsTaTe_3$. This study was performed with the use of a Siemens D5000 powder diffractometer with graphite monochromated Cu Kα radiation. Finely powdered $CsTaTe_3$ was applied to a Pt/Rh heating strip of a Buhler HDK S1 high-temperature attachment. Under a He atmosphere the sample was heated from 298 to 673 K at 20 K intervals and was held at each temperature for 15 min prior to data collection. X-ray diffraction patterns were recorded from 10 to 80° in 2θ with a step size of 0.04° and a counting time of 1.5 s.

Extended Hückel and DFT Calculations. Extended Hückel calculations on both molecular and one-dimensional substructures were carried out with YAeHMOP.[27] The weighted Wolfsberg−Helmholz formula for the off-diagonal Hamiltonian matrix elements was employed.[28] The atomic parameters (orbital energies and Slater exponents)[29] used in our calculations are listed in Table 4. A 100 k-point set was used to compute average properties of the $^1_\infty[TaQ_3^-]$ chains. The geometry of the TaQ_6^{7-} units and $^1_\infty[TaQ_3^-]$ chains was taken from the corresponding $CsTaQ_3$ structures. DFT calculations were carried out at the LDA level with the use of the Plane-Wave package[30,31] with Troullier−Martins pseudopotentials.[32−34] A 6 k-point set was used for geometry optimization.

Results and Discussion

Description of the Structure. The isostructural compounds $CsTaQ_3$ (Q = S, Se, and Te) have the $BaVS_3$[5] structure type. $CsTaTe_3$ is the first ternary alkali-metal or alkaline-earth-metal group-V telluride. As the shortest Q−Q interactions (Table 3) are 3.379(9) Å in $CsTaS_3$, 3.609(3) Å in $CsTaSe_3$, and 3.964(2) Å in $CsTaTe_3$, the formal oxidation states Cs^+, Ta^{5+}, S^{2-}, Se^{2-}, and Te^{2-} may be confidently assigned. The crystal structures of $CsTaQ_3$ comprise a hexagonal stacking of CsQ_3 planes (similar to the (111) planes found in the perovskite structure) with one quarter of the interlayer octahedral sites (all of those surrounded by Q^{2-} anions exclusively) occupied by Ta^{5+} cations. Whereas the octahedra in the cubic-close-packed perovskite structure are linked by vertex sharing, the octahedra in the hexagonal variant $BaVS_3$ structure share faces along the [001] direction. Thus $^1_\infty[TaQ_3^-]$ chains of face-sharing Ta-centered octahedra are present in the $CsTaQ_3$ structure (Figure 1). That $CsTaTe_3$ exhibits this structure type is surprising in light of the dearth of tellurides that feature face-sharing octahedra.

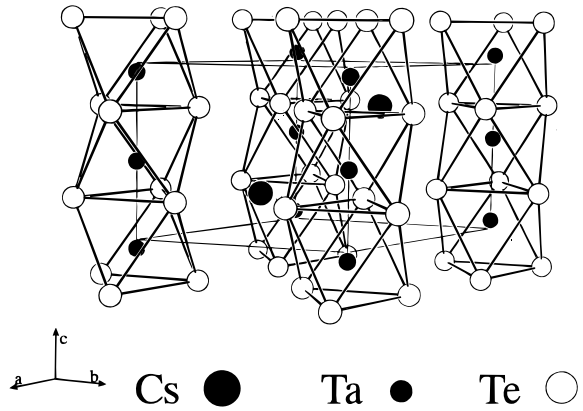

Figure 1. Unit cell of $CsTaTe_3$. Here and in the succeeding figure atoms are drawn as circles of arbitrary size. The Ta atoms are displaced from the centers of the TaQ_6 octahedra with equal probability "up" or "down" along the *c* axis.

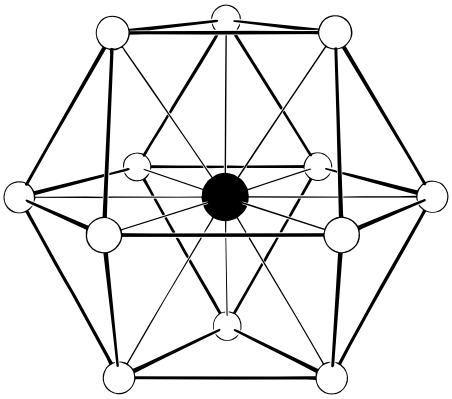

Figure 2. Anticubooctahedral coordination about the Cs^+ cations in $CsTaQ_3$.

The Cs^+ cations that separate the chains exhibit 12-fold anticubooctahedral coordination to Q^{2-} anions at distances of 3.636(1) and 3.731(3) Å for $CsTaS_3$, 3.751(1) and 3.821(1) Å for $CsTaSe_3$, and 3.996(2) and 4.004(2) Å for $CsTaTe_3$ (Figure 2). These are comparable to the Cs−Q interactions found in the structures of $Cs_2B_2S_4$ (3.659(1) to 3.768(1) Å),[35] $CsCuSe_4$ (3.617(1) to 3.768(1) Å),[36] and $Cs_2Ag_2ZrTe_4$ (3.878(3) to 3.960(3) Å).[37] The small range of Cs−Q and Q−Q separations in these structures indicates that they are based on a near hexagonal-closest-packing of Q^{2-} anions with interlayer Q−Q and Cs−Q contacts slightly shorter than intralayer ones. $BaVS_3$ has similar packing efficiency with Ba−S interatomic distances ranging from 3.362(3) to 3.418(3) Å and S−S interatomic distances ranging from 3.340(2) to 3.404(2) Å.

Displacement of the Ta Centers. The Ta centers are displaced about the $\bar{3}m$ site along the [001] direction creating two discrete sets of Ta−Q bond distances (2.339(5) and 2.582(6) Å in $CsTaS_3$, 2.440(2) and 2.767(2) Å in $CsTaSe_3$, and 2.616(3) and 2.997(3) Å in $CsTaTe_3$). If the Ta atoms were centered in their Q_6 octahedra, the Ta−Q bond distances would

(27) Landrum, G. *Yet Another extended Hückel Molecular Orbital Package (YAeHMOP)*, **1996**. This software is freely available on the World Wide Web at http://overlap.chem.cornell.edu:8080/yaehmop.html.
(28) Ammeter, J. H.; Bürgi, H.-B.; Thibeault, J. C.; Hoffmann, R. *J. Am. Chem. Soc.* **1978**, *100*, 3686−3692.
(29) Tables of Parameters for Extended Hückel Calculations; collected by Alvarez, S., Universitat de Barselona, 1993.
(30) Teter, M. P.; Payne, M. C.; Allan, D. C. *Phys. Rev. B* **1989**, *40*, 12255−12263.
(31) Payne, M. C.; Teter, M. P.; Allan, D. C.; Arias, T. A.; Joannopoulos, J. D. *Rev. Mod. Phys.* **1992**, *64*, 1045−1097.
(32) Troullier, N.; Martins, J. L. *Solid State Commun.* **1990**, *74*, 613−616.
(33) Troullier, N.; Martins, J. L. *Phys. Rev. B* **1991**, *43*, 1993−2006.
(34) Troullier, N.; Martins, J. L. *Phys. Rev. B* **1991**, *43*, 8861−8869.
(35) Hammerschmidt, A.; Jansen, C.; Küper, J.; Püttmann, C.; Krebs, B. *Z. Anorg. Allg. Chem.* **1995**, *621*, 1330−1337.
(36) Hartig, N. S.; Dorhout, P. K.; Miller, S. M. *J. Solid State Chem.* **1994**, *113*, 88−93.
(37) Pell, M. A.; Ibers, J. A. *J. Am. Chem. Soc.* **1995**, *117*, 6284−6286.

be 2.455, 2.594, and 2.794 Å for $CsTaS_3$, $CsTaSe_3$, and $CsTaTe_3$, respectively. When the Ta−Q distances in the $CsTaQ_3$ structures are compared with those in the structures of the octahedral Ta^{5+} compounds $CuTaS_3$ (2.282(4) to 2.683(4) Å),[38] Ta_2NiSe_7 (2.473(2) to 2.720(2) Å),[39] Ta_2PtSe_7 (2.482(3) to 2.700(3) Å),[39] $Ta_4Pd_3Te_{16}$ (2.662(1) to 2.899(1) Å),[40] $Ta_3Pd_3Te_{14}$ (2.644(4) to 2.894(4) Å),[41] and $TaIrTe_4$ (2.646(3) to 2.888(3) Å),[42] it is apparent that the Ta−Q bond distances in the *undistorted* structure models are more typical than those in the observed structures. This observation has been confirmed with bond valence calculations on the *undistorted* structure models with the use of the program EUTAX.[43,44]

Note that only the Ta^{5+} centers are displaced in the $CsTaQ_3$ structures; the Cs^+ and Q^{2-} ions reside on the same respective Wyckoff positions as the Ba^{2+} and S^{2-} ions in the $BaVS_3$ structure. What is the reason for the Ta^{5+} displacements? There are several possible explanations. For instance, charge-density-wave transitions in one-dimensional Nb and Ta chalcogenides are well documented.[45,46] Crystallographic refinements of the atomic occupancy factors and elemental analysis by EDX suggest, but do not prove, that the present compounds are stoichiometric and do not contain appreciable percentages of Ta^{4+} centers. Magnetic data indicate that $CsTaTe_3$ is diamagnetic, consistent with a d^0 configuration for Ta. The value of χ at 300 K is -7.1×10^{-5} emu. The weak temperature and field dependence observed are ascribed to a small amount of paramagnetic impurity. Thus a Peierls distortion is unlikely. Distorted octahedral structures involving Ta^{5+} and other d^0 metal cations are fairly common; these distortions have been attributed by Kunz and Brown[47] to a variety of effects, including net stabilization of nearest neighbor networks, lattice stresses, cation−cation repulsions, and second-order Jahn−Teller distortions (an electronic effect that we discuss below).

Attempts to refine the present structures in the noncentrosymmetric space group $P6_3mc$ were not successful. Refinements of inversion and merohedral twinning models in space group $P6_3mc$ led to markedly poorer agreement indices than did refinements of the untwinned models in space group $P6_3/mmc$. It thus seems that these structures are centrosymmetric, and this implies that on average the Ta atoms are equally displaced on either side of the 0,0,0 position along [001]. This could arise from purely random displacements of the Ta centers in each chain. This would lead to a random distribution along a chain of three different Ta−Ta separations (2.579(12), 2.980(12), and 3.382(12) Å in $CsTaS_3$, 2.540(5), 3.091(5), and 3.642(5) Å in $CsTaSe_3$, and 2.590(6), 3.248(6), and 3.906(6) Å in $CsTaTe_3$). Note the shorter of each of these interactions is very short indeed, among the shortest that have been observed, and this makes such a model unlikely. For example, consider the following Ta−Ta separations: $BaTa_{0.8}Se_3$, 3.015 Å;[3] $BaTaS_3$, 2.872(3) Å;[10,11] Ta_6S, 2.644(5) Å;[48] [(cb)$(PMe_2Ph)_2$(H)Ta(μ-H)$_4$Ta(H)$(PMe_2Ph)_2$(cb)] (cb = carbazole), 2.536(1) Å;[49] and $Ta_2Cl_4(PMe_3)_4H_4$, 2.511(2) Å.[50] In addition to this random distribution along a given chain, there are ordered ways that lead to a centrosymmetric structure. In one, pairs of Ta atoms could cluster together (the "pairing distortion"), much as in materials that have undergone a Peierls distortion. There result two distinct Ta−Ta separations, the same as the shortest and the longest Ta−Ta separations in the random distribution model mentioned above. In this model there must be no interchain communication or a doubling of the c axis would result. No evidence for a $2c$ supercell could be observed on overexposed oscillation photographs taken at room temperature of a crystal of $CsTaTe_3$ mounted along [001]. This pairing model seems unlikely because very short Ta−Ta separations are involved and because no such pairing has been detected in the structures of the Ta^{5+} compounds $BaTa_{0.8}S_3$ and $BaTa_{0.8}Se_3$[3] or in the Ta^{4+} compound $BaTaS_3$,[9] although in this instance their electronic structures suggest that such distortions would be favorable.[11,51,52] In the most likely model, favored both by geometrical considerations and by extended Hückel calculations (see below), the Ta atoms in a given chain could all shift in the same direction (the "sliding distortion") with the result that individual $^1_\infty[TaQ_3^-]$ chains are polar. Very weak interchain communication[53] would result in equal numbers of chains of each polarity and a centrosymmetric structure in which Ta−Ta separations were normal, namely 2.980(1), 3.091(1), and 3.248(2) Å in $CsTaS_3$, $CsTaSe_3$, and $CsTaTe_3$, respectively. These Ta−Ta interactions are below the critical distance required for extended metal−metal overlap along the chain axes.[54] But $CsTaSe_3$ is an insulator with an electrical conductivity less than 6.8×10^{-7} Ω^{-1} cm^{-1} at 77 K and $CsTaTe_3$ is a semiconductor with an electrical conductivity of 5.4×10^{-3} Ω^{-1}cm^{-1} at 300 K and 4.3×10^{-3} Ω^{-1} cm^{-1} at 77 K. Yet, semiconducting behavior is observed in $BaTaS_3$,[11] $BaTa_{0.8}S_3$,[3] and $BaTaSe_3$[10] despite short Ta−Ta separations.

We now consider what we can learn through the use of the extended Hückel method[55,56] about why there are Ta displacements in the $^1_\infty[TaQ_3^-]$ chains and which of the two possible patterns of Ta displacements, namely the pairing distortion or the sliding distortion, is more likely. First, the electronic structure of an isolated TaQ_6^{7-} unit (with formally Ta^{5+} and Q^{2-} centers) will be discussed. This allows us to identify the molecular orbitals that are responsible for the second-order Jahn−Teller distortion[57] of Ta along the $\bar{3}$ axis of a TaQ_6^{7-} unit. The results presented were obtained for $CsTaQ_3$ with Q = Te. Figure 3 schematically presents the molecular orbitals of a $TaTe_6^{7-}$ unit, the Te atoms forming a trigonal antiprism (nearly an octahedron). The effect of the Ta distortion from the center of the trigonal antiprism along the C_3 axis is displayed

(38) Sunshine, S. A.; Ibers, J. A. *Acta Crystallogr., Sect. C: Cryst. Struct. Commun.* **1987**, *43*, 1019−1022.
(39) Sunshine, S. A.; Ibers, J. A. *Inorg. Chem.* **1986**, *25*, 4355−4358.
(40) Mar, A.; Ibers, J. A. *J. Chem. Soc., Dalton Trans.* **1991**, 639−641.
(41) Liimatta, E. W.; Ibers, J. A. *J. Solid State Chem.* **1989**, *78*, 7−16.
(42) Mar, A.; Jobic, S.; Ibers, J. A. *J. Am. Chem. Soc.* **1992**, *114*, 8963−8971.
(43) Brese, N. E.; O'Keeffe, M. *Acta Crystallogr., Sect. B: Struct. Sci.* **1991**, *47*, 192−197.
(44) O'Keeffe, M.; Brese, N. E. *J. Am. Chem. Soc.* **1991**, *113*, 3226−3229.
(45) Prodan, A.; Marinkovic, V.; Boswell, F. W.; Bennett, J. C.; Remskar, M. *J. Alloys Compd.* **1995**, *219*, 69−72.
(46) Meerschaut, A.; Gressier, P.; Guemas, L.; Rouxel, J. *J. Solid State Chem.* **1984**, *51*, 307−314.
(47) Kunz, M.; Brown, I. D. *J. Solid State Chem.* **1995**, *115*, 395−406.
(48) Franzen, H. F.; Smeggil, J. G. *Acta Crystallogr., Sect. B: Struct. Crystallogr. Cryst. Chem.* **1970**, *26*, 125−129.
(49) Profilet, R. D.; Fanwick, P. E.; Rothwell, I. P. *Polyhedron* **1992**, *11*, 1559−1561.
(50) Scioly, A. J.; Luetkens, M. L., Jr.; Wilson, R. B., Jr.; Huffman, J. C.; Sattelberger, A. P. *Polyhedron* **1987**, *6*, 741−757.
(51) Whangbo, Myung-H.; Foshee, M. J.; Hoffmann, R. *Inorg. Chem.* **1980**, *19*, 1723−1728.
(52) Peierls, R. E. *Quantum Theory of Solids*; Oxford University Press: London, 1955.
(53) The interchain dipolar interactions are estimated to be less than 1.0 $\times$ 10^{-5} eV for the chains with the sliding distortion and less than 1.0 $\times$ 10^{-2} eV for the chains with the pairing distortion.
(54) Goodenough, J. B., Ed. *Magnetism and the Chemical Bond*; John Wiley & Sons: New York and London, 1963.
(55) Hoffmann, R. *J. Chem. Phys.* **1963**, *39*, 1397−1412.
(56) Hoffmann, R.; Lipscomb, W. N. *J. Chem. Phys.* **1962**, *36*, 2179−2189.
(57) Albright, T. A.; Burdett, J. K.; Whangbo, M.-H. *Orbital Interactions in Chemistry*; Wiley: New York, 1985.

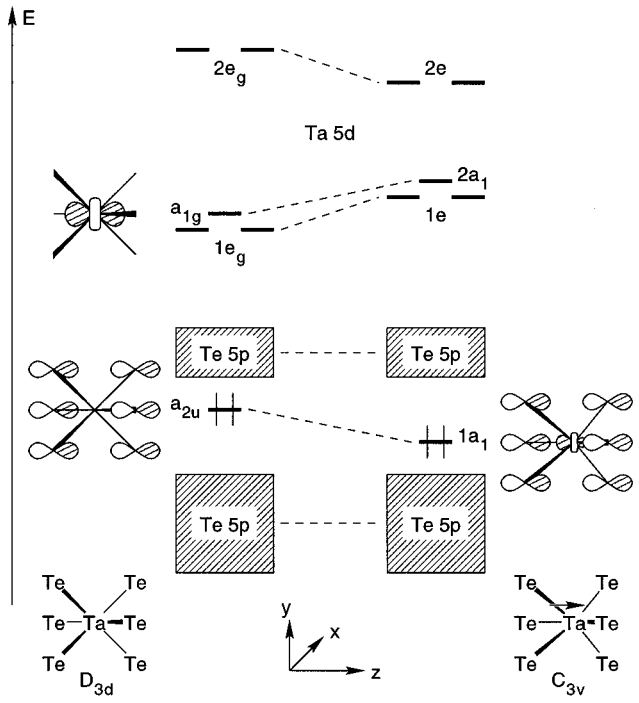

Figure 3. Walsh diagram for the Ta displacement along the z axis in a $TaTe_6^{7-}$ unit.

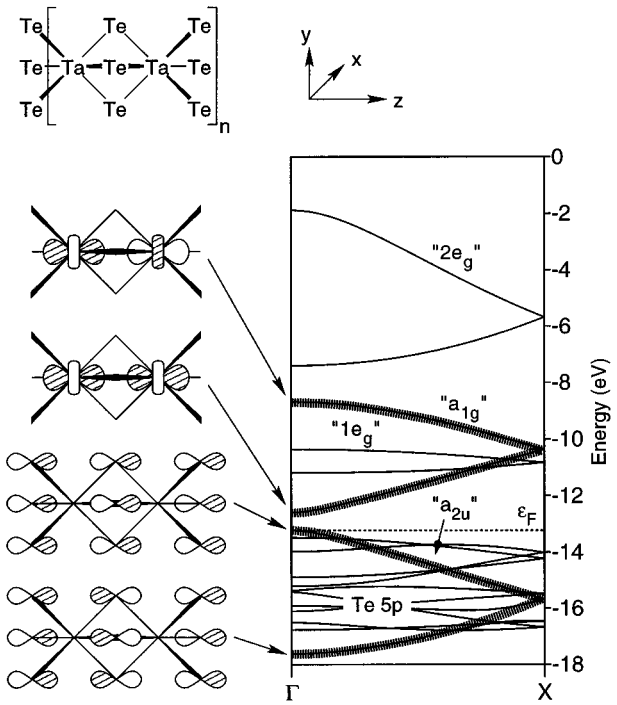

Figure 4. Band structure for an undistorted $^1_\infty[TaTe_3^-]$ chain. The Ta d_{z^2} band and the Te p_z band are emphasized; the corresponding crystal orbitals at the Γ point are shown.

in the form of a Walsh diagram.[58] The energy window is chosen in such a way that only the Ta d orbitals and Te p orbitals are shown. The splitting of the Ta d block, three below two, is consistent with the nearly octahedral coordination. All Te orbitals are filled and all Ta orbitals are empty, in accord with the Ta^{5+}/Te^{2-} formalism.

In seeking an explanation for the deformation observed, we are led to focus on a particular orbital from the Te p-block of a_{2u} symmetry in the undistorted ($\bar{3}$m, D_{3d}) $TaTe_6^{7-}$ unit. This orbital consists mainly of Te p_z orbitals with a small contribution of Ta p_z. It undergoes the largest change in energy among all Te orbitals when the Ta is displaced by 0.329 Å, the experimentally observed value for $CsTaTe_3$. The reason for the stabilization of this orbital is to be found in the mixing in of the empty Ta d_{z^2} orbital. The latter orbital belongs to the a_{1g} irreducible representation in the undistorted fragment, but transforms as a_1 when the symmetry is lowered to C_{3v} (3m). This allows for Ta d_{z^2} mixing into the formerly a_{2u} orbital, which also transforms as a_1 in the distorted fragment. As a result of such mixing, this orbital acquires 4.2% Ta d_{z^2} character and is stabilized by 0.122 eV, equal to 65% of the decrease in the total energy of $TaTe_6^{7-}$.

Now consider the electronic structure of an undistorted $^1_\infty[TaTe_3^-]$ chain, as well as changes that result from the Ta displacement. The band structure of an undistorted $^1_\infty[TaTe_3^-]$ chain is shown in Figure 4.[59] Again we are interested in the Ta d and Te p blocks of orbitals. The former are empty and the latter are occupied with a gap in between, consistent with semiconducting behavior of $CsTaTe_3$. The Ta d bands have been discussed previously in detail.[51,60,61] A feature of the band structure worth noting is the "folded-back" nature of all bands owing to the doubling of the unit cell and the presence of a 6_3 axis. The bands largely responsible for the geometry are related to those in the isolated $TaTe_6^{7-}$ unit: a mainly Ta d_{z^2} band and a mainly Te p_z band.[62] Figure 5 shows the result of Ta d_{z^2} mixing into the top of the Te p_z band for the pairing and the sliding distortions. Note that only the *top* of the Ta d_{z^2} band can mix into the Te p_z band when the pairing distortion takes place, whereas the *bottom* of the Ta d_{z^2} band is involved in the sliding distortion. From the point of view of perturbation theory given two otherwise similar orbital interactions, the strength of the interaction is inversely proportional to the energy difference between the interacting levels.[57] Therefore stronger Ta d_{z^2} mixing is expected for the sliding distortion, along with more substantial stabilization of the top of the Te p_z band. Indeed, the Ta d_{z^2} band constitutes 17.7% of the top of the Te p_z band after the sliding distortion, whereas only 5.4% of the Ta d_{z^2} band mixes into the top of the Te p_z band after the pairing distortion.

Note that among all possible Ta distortion patterns the sliding distortion provides the most effective interaction between the two bands because it involves the parts of the bands that are closest in energy. The Te s bands are also affected by the Ta displacement. Mixing of the empty Ta states (allowed owing to a lowering of symmetry) takes place in both of the distorted structures to a similar extent because the Te s bands are rather far in energy from the empty Ta states.

There is one more effect at work when Ta centers are paired. Owing to the loss of the screw axis, bands do not meet at the X point so the folded-back nature of the band structure is lost. This would lead to stabilization for a half-filled band because its lower filled half would be stabilized around X and its upper unfilled half would be destabilized at X; a Peierls distortion would result. However, when the band in question is completely filled, then the destabilization of the upper, now filled, half more

(58) A number of distortions for d^0 transition metal complexes are discussed in ref 66.

(59) For a general discussion of chemical bonding in extended structures see refs 67 and 68.

(60) Lachgar, A.; Dudis, D. S.; Dorhout, P. K.; Corbett, J. D. *Inorg. Chem.* **1991**, *30*, 3321−3326.

(61) Dorhout, P. K.; Corbett, J. D. *Inorg. Chem.* **1991**, *30*, 3326−3333.

(62) There are several bands that are mostly Te p_z in character, but we are interested in the one symmetric with respect to the C_3 axis. This is the band that we will refer to as the "Te p_z band".

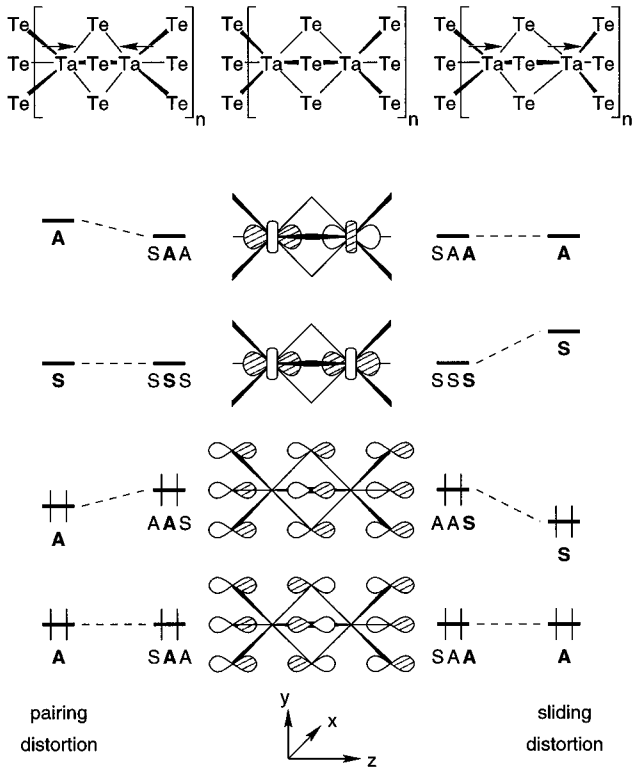

Figure 5. The effect of the pairing and sliding distortions on the Ta d_{z^2} and Te p_z bands at the Γ point. The symmetry labels are assigned with respect to the following symmetry operations: σ_{xy} containing Ta, σ_{xy} containing Te, and 6_3 screw axis along z. Only the σ_{xy} containing Te is retained after the pairing distortion; only the 6_3 screw axis is retained after the sliding distortion.

than outweighs the stabilization provided by the lower half.[63] A similar situation takes place at the Γ point: every filled Te band contributes to destabilization because the states at the top and the bottom of the band can interact with each other. For example, Figure 5 shows that the symmetry of the Te p_z band is the same at the top and at the bottom of the band. Such intraband[64] interaction takes place in the rest of the Brillouin zone as well. There is no intraband interaction in the case of the sliding distortion.

To summarize, the sliding distortion in a $^1_\infty[TaTe_3^-]$ chain leads to a substantial stabilization of the top of the filled Te p_z band, other Te p bands being relatively unaffected. The Te s bands are also stabilized. The pairing distortion provides a small stabilization of the top of the Te p_z band. The intraband interactions result in destabilization that outweighs the stabilization resulting from the second-order Jahn−Teller mixing in both the Te s and the Te p blocks. The computed changes in the total energy of the chain are +0.071 eV/Ta (net destabilization) for the pairing distortion and −0.484 eV/Ta (net stabilization) for the sliding distortion. The stabilization of the top of the Te p_z band after the sliding distortion amounts to 60% of the total energy decrease.

Similar results were obtained for $CsTaQ_3$, Q = S or Se. For Q = S there is a small overlap between the Ta d_{z^2} band and the block of the Te p bands in the undistorted $^1_\infty[TaS_3^-]$ chain. This, however, has no significant effect on the energetics of the Ta distortions. We also carried out calculations on the full three-dimensional $CsTaQ_3$ structures; the results show that the inclusion of interchain interactions and the Cs cations does not change the conclusions obtained for the isolated chains.

Sometimes the extended Hückel method fails to reproduce bond lengths when it is allowed to optimize geometry.[65] One must take care when comparing total energies of structures with different bond lengths. In the present instance when the Ta distortion along the $\bar{3}$ axis in the $TaTe_6^{7-}$ unit is optimized, an unreasonable distortion of 1.46 Å is predicted. But the goal of our analysis is not to predict quantitatively to what extent a distortion occurs, but rather to give qualitative arguments as to what may be the cause for the experimentally observed distortion and then to use similar arguments to decide which distortion pattern is more likely. We expect our prediction that the sliding distortion is more energetically favorable than the pairing distortion to be correct because the two geometries feature identical Ta−Te bond lengths.

We attempted DFT calculations in order to compare energies of $CsTaQ_3$ structures with the sliding and pairing distortions, as well as with undistorted $^1_\infty[TaQ_3^-]$ chains. Only $CsTaS_3$ with the sliding distortion was found to have a small band gap of 0.156 eV above the Fermi level. In all the other eight systems the Ta d bands were found to overlap a little with the Te p bands. Calculations on metallic systems cannot be carried out with the current version of the program, so no further studies on the latter systems were done. Geometry optimization was attempted for the $CsTaS_3$ structure with all Ta centers displaced in the same direction and with the cell parameters fixed. The resulting Ta position of (0,0,0.0347) is very close to the experimentally observed value of (0,0,0.0337). The calculated Cs and S positions are also virtually identical with those derived from the X-ray data. The fact that the sliding distortion in $CsTaS_3$ corresponds to a local energy minimum is not the absolute proof, but is a strong indication that this distortion correctly describes the structure of $CsTaQ_3$.

Other Observations. DSC measurements have established that $CsTaTe_3$ undergoes an endothermic phase transition at approximately 493 K. There is an irreversible exotherm at approximately 400 K, the source of which is not clear. TGA measurements indicate that the mass loss at 393 K is less than 0.5% whereas the total mass loss by 793 K is only 2.2%. X-ray powder diffraction patterns of $CsTaTe_3$ obtained at temperatures ranging from 298 to 673 K confirm the occurrence of a phase transition at ≈493 K. The structure of the high-temperature phase, which appears to be of lower symmetry, is still under investigation. $BaVS_3$ undergoes a hexagonal to orthorhombic phase transition at 250 K. In its hexagonal phase $BaVS_3$ is a semiconductor, but it becomes metallic at temperatures below 130 K.[5]

Preliminary efforts to synthesize the Nb analogue of $CsTaTe_3$ yielded only $NbTe_2$, Cs_2Te_n, Nb, and Te. Materials of the formula $KMTe_3$ (M = Nb and Ta) could not be isolated.

Acknowledgment. We thank Dr. Björn Borup and Prof. Malcolm H. Chisholm of Indiana University for acquiring the DSC and TGA data and Drs. Michael F. Mansuetto and Michael M. Thackeray of Argonne National Laboratory for collecting the high-temperature X-ray powder diffraction data. At Northwestern University this work was supported by NSF Grant No.

(63) When two orbitals interact, the antibonding combination is more destabilized than the bonding combination is stabilized. See ref 57.

(64) By intraband interaction we mean interaction between the two halves of a folded-back band.

(65) Lowe, J. P. *Quantum Chemistry*, 2nd ed.; Academic Press, Inc. Harcourt Brace & Company: Boston, 1993.

(66) Kang, S. K.; Tang, H.; Albright, T. A. *J. Am. Chem. Soc.* **1993**, *115*, 1971−1981.

(67) Hoffmann, R. *Solids and Surfaces: A Chemist's View of Bonding in Extended Structures*; VCH Publishers: New York, 1988.

(68) Burdett, J. K. *Chemical Bonding in Solids*; Oxford University Press: New York, 1995.

(69) Huffman, J. C. Ph.D. Dissertation, Indiana University, 1974.

DMR 91-14934, and use was made of MRL Central Facilities supported by the National Science Foundation at the Materials Research Center of Northwestern University under Grant No. DMR 91-20521. G.V.M.V. would like to thank Prof. Roald Hoffmann, Ms. Erika Merschrod, and Dr. Christopher L. Henley for their comments, the Olin Foundation for support through a fellowship, and the National Science Foundation for support through Grant No. CHE 94-08455.

Supporting Information Available: Tables of data and details of crystal structure determinations, bond lengths and angles, and aniostropic displacement parameters (16 pages). See any current masthead page for ordering and Internet access instructions.

JA964473A